FULL RESEARCH ARTICLE

Isocyanate-free urethanediol itaconates as biobased liquid monomers in photopolymerization-based 3D printing

Rosario Carmenini[1] · Chiara Spanu[1] · Erica Locatelli[1] · Letizia Sambri[1] · Mauro Comes Franchini[1] · Mirko Maturi[1]

Abstract

Nowadays, most of the commercial resins for VP are composed of (meth)acrylated urethanes, as they are cheap and provide good mechanical properties to the thermosets produced by their photocuring. However, such urethanes are still produced using toxic and polluting isocyanates, though alternative pathways exploiting cyclic carbonates and biobased amines are arising. Unfortunately, the use of biobased amines and carbonates to produce (meth)acrylate urethanes often leads to the formation of solid products that display poor solubility in the liquid components of photocurable resins. In this work, we describe the synthesis of fully biobased diurethanediols using a biobased diamine and bioderived carbonates functionalized with itaconic acid moieties that are liquid at room temperature and that can be efficiently formulated with (meth)acrylic and itaconic acid-based formulations for VP leading to 3D printed materials with good mechanical properties, comparable to those of commercially available non-biobased alternatives. In fact, depending on the resin formulations, the addition of diurethanediols diitaconates led to the obtainment of 3D printed materials with elastic moduli as high as 1 GPa, and tensile strengths over 30 MPa, and biobased contents as high as 90 wt.%. These products may serve as candidates for the replacement of isocyanate-based components with the aim of increasing the sustainability of resins' manufacturing for VP.

Keywords Non-isocyanate urethanes · Itaconic acid · VAT photopolymerization · Biobased materials · Additive manufacturing

1 Introduction

The basic principle of additive manufacturing, also known as 3D printing, is building up an object layer by layer; in a first stage, the design of the desired object is created by computer-aided design (CAD) and the virtual model is then digitally sliced into horizontal layers for a printable command sequence. Via a command file usually named G-code, the virtual coordinates are sent to the 3D printer, which deposits the material in predesigned locations at the x–y plane and the entire process is repeated along the z-axis. Compared to traditional manufacturing techniques, modifications in the shape of the 3D printed manufactures can be easily done by modifying the digital object, without the need for unique tools for a single modification [1]. Furthermore, 3D printing is a sustainable manufacturing process, as additive fabrication results in much less material waste [2]. Among the different technologies, vat photopolymerization (VP) allows to produce three-dimensional objects by selectively photocuring monolayers of a monomeric resin into layered 3D

✉ Mauro Comes Franchini
mauro.comesfranchini@unibo.it

✉ Mirko Maturi
mirko.maturi@uca.es

Rosario Carmenini
rosario.carmenini2@unibo.it

Chiara Spanu
chiara-spanu3@unibo.it

Erica Locatelli
erica.locatelli2@unibo.it

Letizia Sambri
letizia.sambri@unibo.it

1 Department of Industrial Chemistry "Toso Montanari", University of Bologna, Via P. Gobetti 85, 40129 Bologna, Italy

objects [3–5]. The use of high-resolution UV light sources for triggering the spatially controlled photopolymerization of the resins enabled the manufacturing of objects with small details at resolutions of the order of tens of microns, depending on the available implementation [6]. Moreover, the limited price of the required equipment has made VP the first high-resolution 3D printing technique available for private consumers' and everyday use [7, 8]. In addition, by selecting the appropriate monomers to be formulated into the photocurable resin, it is possible to obtain materials spanning over a large range of mechanical, thermal, optical and electrical properties, allowing to employ VP in a great variety of high added value applications, such as for biomedical, dental, jewelry and aerospace [9–11], with potential applications spanning from stimuli-responsive materials to tissue engineering [12, 13]. Thanks to its important contribution to the good mechanical properties of 3D printed materials, one of the most commonly employed monomers for producing VP resins is (7,9,9-trimethyl-4,13-dioxo-3,14-dioxa-5,12-diaza-hexadecane-1,16-diylbis(2-methylacrylate), known simply as urethane dimethacrylate, produced by reacting a difunctional aliphatic isocyanate with 2-hydroxyethyl methacrylate [14–16]. In the industrial sector, the synthesis of isocyanates poses a significant hazard not only in terms of the isocyanates themselves, but also concerning the substrates used in their production; on an industrial scale, in fact, isocyanates are obtained through the phosgene route [17]. Owing to the increasing concerns related to the environmental impact of isocyanates and their production processes, the scientific community has developed alternative routes for the production of urethanes and polyurethanes by aminolysis of cyclic carbonates, obtained in turn by reacting bioderived epoxides with CO_2 [18, 19]. Considerable research efforts have been devoted to exploring the potential of carbon dioxide as a renewable C1 building block for chemical synthesis. The rationale behind this stems from the fact that CO_2 is abundant, readily available, non-toxic, and non-flammable, making it an attractive and cost-effective source for the production of chemical products [20]. On the other hand, biobased epoxides can be synthesized from waste vegetable oils via epoxidation, which not only provides a sustainable alternative to traditional petroleum-based epoxides, but also utilizes a waste product, helping to reduce environmental impact [21]. By combining bifunctional primary amines with monofunctional cyclic carbonates such as ethylene carbonate (EC) and propylene carbonate (PC), it is possible to produce diurethanediols (UDOs), which have been previously employed for the preparation of poly(ester urethane)s [22, 23]. The diamines can be selected in the pool of biobased diamines which include 1,3-propanediamine, 1,4-butanediamine, and 1,5-pentanediamine, obtained by decarboxylation of lysine, arginine, and ornithine, respectively [24]. Furthermore, UDOs have been recently employed as additives in VP after

functionalizing the alcoholic termini with methacrylate residues [25]. However, the efforts towards an increase in the sustainability of VP resins were limited by the use of methacrylic acid as the photocurable moiety, and the incorporation of diamines from non-renewable resources. Disappointingly, the produced methacrylated UDOs were solid at room temperature, thus limiting their applicability for applications in VP. Currently, the most promising candidate that is emerging as a biobased alternative for replacing (meth)acrylic acid functionalities in photocurable mixtures is indeed itaconic acid, or 4-methylenesuccinic acid. Traditionally produced by distillation of citric acid, itaconic acid is nowadays produced by direct fermentation of glucose-containing biomasses by specifically engineered bacterial strains. [26]. Many examples of the incorporation of itaconic acid in resins for VP have been recently reported in the literature, mainly employing its diesters, polyesters, poly(ester-amide)s and poly(ester-thioether)s [27–30]. In a single example available in the literature, biobased UDOs have been polymerized with itaconic acid to produced fully biobased photocurable poly(ester-urethane)s, but their physical properties did not make them suitable for the formulations of 3D printable resins, and they were explored mostly as coating materials [31]. This paper introduces the synthesis and characterization of liquid biobased diurethanediols (UDOs) that have been functionalized with itaconic acid monomethyl ester for use in high precision additive manufacturing applications. The liquid state of the UDO backbones allows them to be combined with high percentages of (meth)acrylic and itaconic acid-based co-monomers, resulting in the development of highly biobased photocurable resins. The addition of UDOs-I has been thoroughly investigated for its impact on the mechanical properties of these resins, including tensile, flexural, and hardness properties, revealing mechanical properties comparable to those of commercially available non-renewable urethane monomer-based alternatives. The biobased content of the prepared formulation has also been evaluated and discussed in relation to the extracted mechanical properties. This research presents a fully biobased building block that can be used in photocurable mixtures for high precision additive manufacturing applications to increase their sustainability without significantly affecting their mechanical properties.

2 Materials and methods

All chemicals were purchased from Sigma-Aldrich (St. Louis, MO, USA) and used as received. Chloroform was dried by distillation over $CaCl_2$ and used promptly. Grindsted Soft-N-Safe (9-hydroxystearic acid monoglyceride triacetate, SNS) was purchased from Danisco (Brabrand, Denmark).

2.1 Synthesis of the diurethanediols bis(hydroxyethyl)butane-1,4-diyl dicarbamate (UDO$_2$) and bis (hydroxypropyl)butane-1,4-diyl dicarbamate (UDO$_3$)

In a 500 mL round-bottomed flask equipped with a large magnetic stirrer 1,4-diaminobutane (DAB, 89.5 g, 1 mol) was added dropwise to 2 mol of the appropriate carbonate (ethylene carbonate, EC, 176 g, for UDO$_2$ and propylene carbonate, PC, 204 g, for UDO$_3$) under a nitrogen atmosphere. The mixture was kept at 80 °C for 1 h to ensure the reaction's completeness. Then, the product was rapidly cooled to room temperature and precipitated with diethyl ether to obtain the desired products as a white solid, which was then filtered and dried. ESI–MS: $[M+Na^+] = 287$ for UDO$_2$ and $[M+Na^+] = 315$ for UDO$_3$. Yield = 92% for UDO$_2$ and 90% for UDO$_3$.

2.2 Synthesis of monomethyl itaconoyl chloride

In a 1 L round-bottomed flask under nitrogen atmosphere equipped with a CaCl$_2$ drying tube, 180 mL of oxalyl chloride (2.1 mol) was added to itaconic acid monomethyl ester (216 g, 1.5 mol). The reaction was allowed to take place by stirring overnight at room temperature. Once the reaction was completed all acid was dissolved, and unreacted oxalyl chloride was distilled at room temperature under high vacuum and recovered for further use. Then, the temperature was increased to 120 °C and pure monomethyl itaconoyl chloride was distilled off as a colorless liquid from the reaction mixture and stored under inert atmosphere in the dark at − 20 °C. ^{1}H NMR (400 MHz, CDCl3) δ 6.72 (s, 1H), 6.18 (s, 1H), 3.72 (s, 3H), 3.40 (s, 2H). Yield = 86%.

2.3 Synthesis of diurethanediols bis(methyl itaconate) (UDO$_2$-I and UDO$_3$-I)

In a three-necked dry 500 mL flask equipped with a large magnetic stirrer and a rubber septum, 200 mL of dry chloroform in which 0.115 mol of UDO$_2$ (28.3 g) or UDO$_3$ (33.4 g) was dissolved was added under a nitrogen flow. Subsequently, 32.5 mL (230 mmol) of triethylamine was added and the mixture was cooled down to 0 °C using an ice bath. Then, 29 mL (0.23 mol) of monomethyl itaconoyl chloride were slowly added dropwise over 1 h using a dropping funnel. When the addition was complete, the ice bath was removed, and the mixture was left under stirring and nitrogen atmosphere for 2 h. The mixture was washed several times with water to remove triethylamine chloride, residual monomethyl itaconoyl chloride, and traces of the corresponding carboxylic acid. Then, the organic phase was dried over Na$_2$SO$_4$ and evaporated to afford the diurethanediol bis(methyl itaconate)s. ESI–MS: $[M+Na+] = 553$ for UDO$_2$-I and $[M+Na+] = 567$ for UDO$_3$-I. Yield = 83% for UDO$_2$-I and 85% for UDO$_3$-I.

2.4 Synthesis of 1,4-butanediyl bis(methyl itaconate)—I$_2$B$_1$

In a 1-L round-bottomed flask, dimethyl itaconate (474 g, 3 mol) and butanediol (132 mL, 1.5 mol) are mixed with 5.25 g (21 mmol) of dibutyltin (IV) oxide. The mixture is heated to 160 °C for 1 h during which the methanol produced by the transesterification reaction is removed by distillation. At the end of the reaction, the mixture is cooled to room temperature, dissolved in ethyl acetate and washed with water three times. The organic phase is therefore dried over sodium sulfate and evaporated to afford I$_2$B$_1$ as a pale-yellow liquid. ^{1}H NMR (400 MHz, CDCl3) δ: 6.32 (2H), 5.71 (2H), 4.15 (4H), 3.76 (3H), 3.69 (3H), 3.33 (4H), 1.72 (4H). ESI–MS $[M+Na+] = 365$. Yield = 87%.

2.5 Formulation of photocurable resins

The synthetized photocurable monomers were mixed with a fixed-speed planetary mixer (Precifluid P-MIX100) for 4 min according to the compositions reported in Table 1, then poured into the 3D printer vat for spatially controlled photopolymerization (Fig. 1). To all formulations were also added ethyl (2,4,6-trimethylbenzoyl) phenylphosphinate (Et-APO, 2.0 wt.%) as the photoradical polymerization initiator, 2-isopropylthioxanthone (ITX, 0.3 wt.%) as the photoabsorber, and 2,6-ditert-butyl-4-methylphenol (BHT, 0.5 wt.%) as the radical trapping stabilizer, while Grindsted Soft-N-Safe (9-hydroxystearic acid monoglyceride triacetate, SNS, 7.2%) was added as the plasticizer.

Table 1 Weight compositions of the prepared photocurable formulations and the corresponding overall biobased contents

Resin	GDMA (%)	GPT (%)	I$_2$B$_1$	UDO$_3$-I	Biobased content (%)
A0	45	45	–	–	29.6
A1	40	40	–	10%	37.1
A2	30	30	–	30%	52.1
A3	20	20	–	50%	67.1
B0	34	34	22%	–	46.1
B1	15	15	10%	50%	74.7
C0	11	11	68%	–	80.7
C1	5	5	30%	50%	89.7

Percentages sum up to 90% because the remaining 10% is composed of the photoinitiating system and the plasticizer
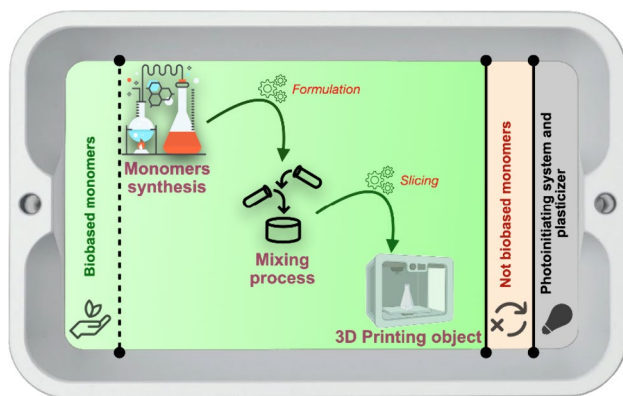
Fig. 1 Schematic representation of the additive manufacturing process employed in this work. Biobased synthetic monomers were firstly synthetized and purified, then they were formulated in concentrations ranging from 10 to 80 wt.% with non-biobased monomers and the photoinitating system. The obtained formulation was then poured into the vat of the 3D printer and selectively photocured into high-resolution biobased polymeric materials

2.6 3D printing of photocurable resins

Dog bones for the tensile test were designed by a computer-assisted design (CAD) following the ISO-37 Type 2 specifications (5×2 mm^2 of section, 25 mm gauge length), and $100 \times 40 \times 10$ mm^3 rectangular bars were designed for three-point bending tests according to ISO 178. The 3D models were sliced using Chitubox v1.7.0 software by importing, at first, the *.stl files corresponding to tensile and bending test specimens onto the virtual plate and then configuring the printing parameters (such as layer height and exposure time) before slicing the final objects for printing into the corresponding g-code. The layer's height was 0.1 mm, while the irradiation time per layer was optimized for each formulation, ranging from 80 to 120 s. The g-codes were then exported into a VP Phrozen Sonic 4 K 3D printer equipped with a 6.1 inch 50 W monochrome 405 nm, ParaLED Matrix 3 UV screen (3840×2160 resolution, 4 K), and the formulated resins were poured into its vat. After the printing, the samples were detached from the build plate and washed with acetone/isopropanol mixture (up to 20 vol.% acetone) to remove the non-polymerized resin, detached from the plate, and dried for 2 h hours at room temperature. Then, 3D printed objects were post-cured at 25 °C for 10 min in a UV curing oven (Sharebot CURE, Nibionno, Italy, $\lambda = 375$–470 nm, 120 W) and exposed to air and environmental light conditions for 1 week prior to mechanical testing. The potential effect of the washing step on the mechanical properties of the photocured materials was assessed by comparing the mechanical properties of washed and unwashed samples, and no appreciable differences were detected.

2.7 Chemical and mechanical characterization

^{1}H and ^{13}C NMR spectra were obtained on Varian Inova (14.09 T, 600 MHz) and Varian Mercury (9.39 T, 400 MHz) NMR spectrometers. In all recorded spectra, chemical shifts were reported in ppm of frequency relative to the residual solvent signals for both nuclei (^{1}H: 7.26 ppm and ^{13}C: 77.16 ppm for CDCl$_3$). ^{13}C NMR analysis was performed using ^{1}H broad band decoupling mode. Mass spectra were recorded on a micromass LCT spectrometer using electro-spray (ES) ionization techniques. ATR–FTIR analysis was performed using a Cary 630 FTIR spectrometer (Agilent). Rotational viscosity measurements were performed on an Anton Paar Rheometer MCR102 with a cone-plate CP50-1 configuration (1° angle and 25 mm diameter). The experiments were achieved with a constant rotational frequency of 1 Hz in the temperature range $+ 10/+ 40$ °C and a heating rate of 5 °C/min. A Remet TC10 universal testing machine was used to perform all the tensile and flexural tests. The instrument was equipped with a 10 N cell, with a crosshead speed of 1 mm min^{-1} for both tests, according to the ISO 37 Type 2 and ISO 178 specifications. Hardness was evaluated using an analogic Shore D durometer (Remet).

3 Results and discussion

Diurethane diols UDO$_2$ and UDO$_3$ were prepared by aminolysis of cyclic carbonates (ethylene carbonate, EC, and propylene carbonate, PC, respectively) using the double-functionalized primary amine 1,4-diaminobutane without the requirement for any solvent. This diamine can be in theory considered as biobased, thanks to the widely explored possibility to obtain it by decarboxylation of the amino acid L-arginine [24, 32]. The aminolysis reaction involves the nucleophilic attack of the amine on the carbonate carbon, leading to the opening of the five-membered ring and the formation of a linear carbamate bearing a free alcoholic group (Scheme 1). To minimize the possibility of the formation of monourethane amines, the diamine was added dropwise into the cyclic carbonate, leading to the immediate formation of urethanediols thanks to the large excess of carbonate at every addition of diamine. Due to the non-selective nature of the aminolysis, the opening of the cyclic carbonates can take place on either side of the C=O; while thanks to the symmetric structure of EC the two possible mechanisms lead to the same product, UDO$_2$, PC aminolysis is expected to lead to the formation of two structural isomers in comparable concentrations [33].

This effect, combined with the bifunctional nature of the selected amine, leads to the formation of UDO$_3$ as three regioisomers: one bearing two secondary OH moieties (UDO$_3$-1), one bearing two primary OH groups (UDO$_3$-2),
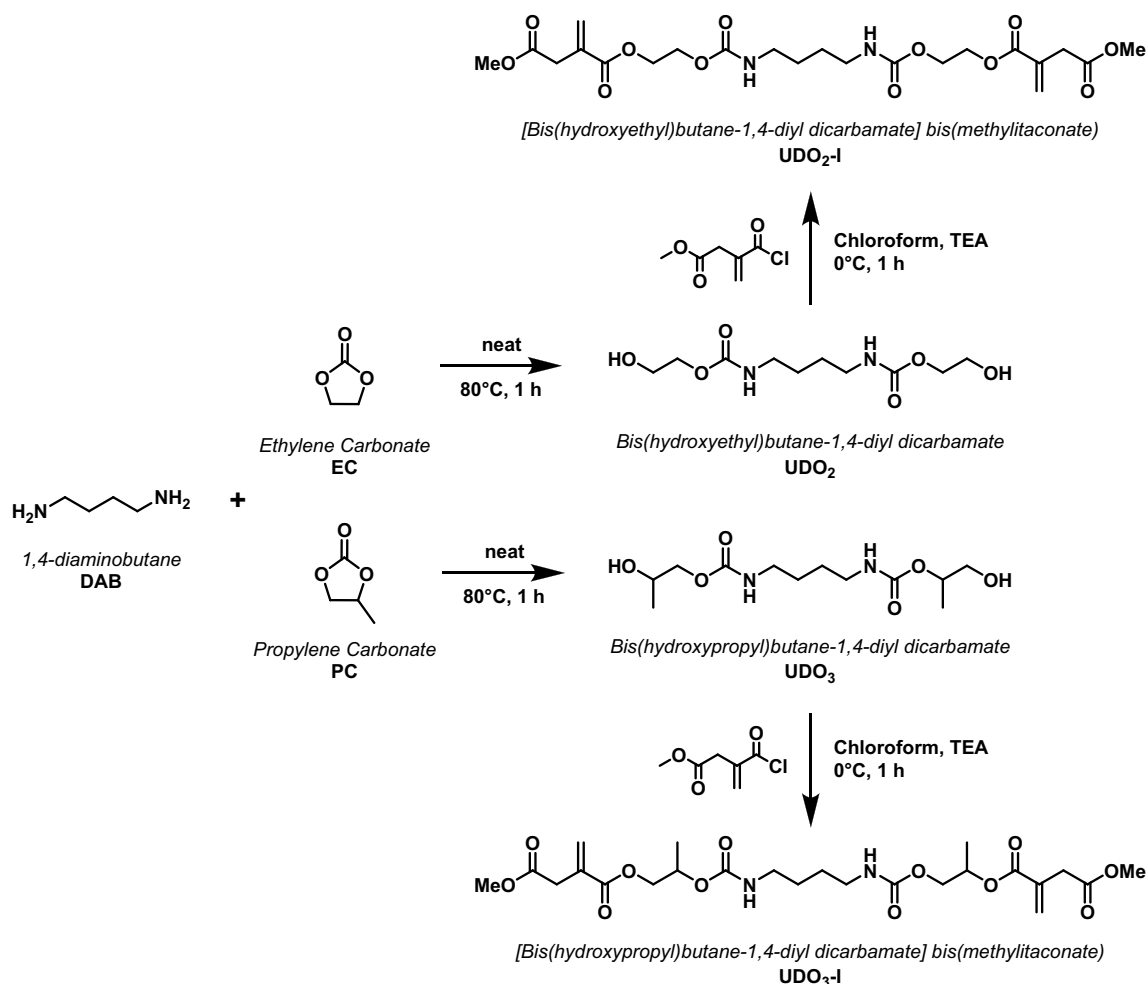
Scheme 1 Synthesis of diurethane diols and their functionalization with itaconic acid moieties to achieve difunctional photocurable UDO$_2$-I and UDO$_3$-I monomers. Due to the non-regioselective nature of the cyclic carbonate opening, all isomers are formed in comparable proportions, but only one of them is depicted here to represent the whole class of isomers

and one bearing one primary and one secondary OH functionalities (UDO$_3$-3) as depicted in Scheme S1. Due to their similar physical–chemical properties, the isomers were not separated and underwent successive functionalization with itaconic acid as a mixture. With respect to UDO$_2$, the product was characterized by ESI–MS and NMR spectroscopy (Figure S1), which confirmed the predicted molecular weight and chemical structure, respectively. Similarly, the outcome of PC aminolysis was confirmed by ESI–MS, which suggested the presence of the diols as the only reaction products, with the expected molecular ion peak common to all regioisomers. ^{1}H–, ^{13}C–, ^{1}H–^{1}H–COSY and ^{1}H–^{13}C–HSQC NMR spectroscopies revealed the presence of all isomers in comparable concentrations, allowing also for the unambiguous assignment of NMR peaks (Fig. 2a, Figure S2-S4 and Table S1). Moreover, by comparing the NMR integrals, it was possible to assess that the aminolysis of PC took place with a preference toward the formation of

the primary alcohol (63%) compared to the secondary alcohol (37%), in agreement with previously published results [34]. Assuming that the regiochemistry of the aminolysis of PC performed by the intermediate monohydroxyurethanes was not dependent on the type of alcoholic functionality formed at first, the UDO$_3$ mixture can be expected to be composed of 14% UDO$_3$-1, 40% UDO$_3$-2, and 46% UDO$_3$-3. Furthermore, ATR–FTIR spectroscopy confirmed the presence of main functional groups expected in the product: N–H/O–H stretching at 3314 cm^{-1}; C–H stretching at 2930–2868 cm^{-1}, carbamate C=O stretching at 1677 cm^{-1}, and N–H bending at 1521 cm^{-1} (Figure S5). Diurethanediol bis(methyl itaconate) UDO$_2$-I and UDO$_3$-I were synthesized by acylation of the corresponding UDO using monomethyl itaconoyl chloride, produced by chlorination of itaconic acid monomethyl ester, as recently reported [35]. The chlorination of monomethyl itaconic acid took place in an excess of oxalyl chloride, and the unreacted chlorinating agent was
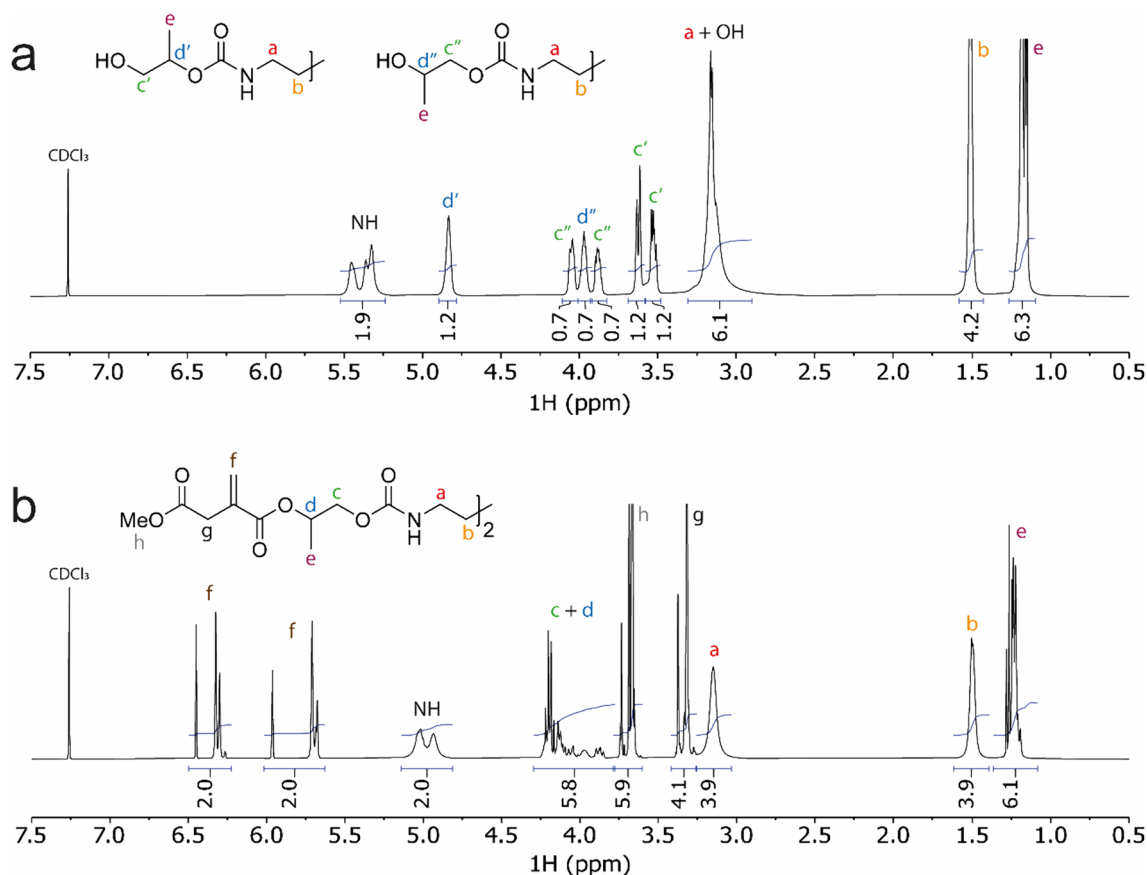
Fig. 2 ¹H-NMR (CDCl₃, 400 MHz) analysis of UDO₃ (**a**) and UDO₃-I (**b**), together with the corresponding signal attributions. For UDO₃-I the structure of only one isomer is reported, but the attribution applies to all nine isomers formed

removed by distillation and recovered for further use. Furthermore, the obtained monomethyl itaconoyl chloride was purified by distillation, allowing for its isolation with high purity. Once isolated, monomethyl itaconoyl chloride was added dropwise to a solution containing triethylamine and the selected UDO to be functionalized, and the esterification reaction took place instantaneously between the itaconic acid chloride and the urethanediols. Such esterification required anhydrous conditions to prevent undesired hydrolysis of the acyl chloride into the corresponding carboxylic acid and the presence of triethylamine that could trap the produced HCl. The expected product structures were confirmed by ESI–MS and NMR spectroscopy (Fig. 2b and Figure S6-S7). Since monomethyl itaconoyl chloride prepared with this method is composed of a mixture of roughly 95% α,β-unsaturated acyl chloride and 5% α,β-unsaturated methyl ester, UDO₃-I is expected to be formed as a mixture of nine isomers where propanediol and itaconic acid residues display all possible orientations. This reflected into highly split NMR signals, which still allowed to confirm the presence of the photocurable moiety of itaconic acid residues and the absence of monosubstituted UDOs derivatives. In addition, ATR–FTIR

spectroscopy (Fig. 3a) was further employed to characterize the functional groups present in UDO₃-I. The first important difference between the prepared itaconic acid-modified diurethanediols lies in their physical state around room temperature. In fact, while UDO₂-I is a solid with a melting temperature significantly above 25 °C, UDO₃-I is a liquid. This is believed to be related to the presence of nine isomers in the product mixture that hinders its assembly and prevents its solidification. To further characterize UDO₃-I on this aspect, its rheological properties were evaluated by measuring its viscosity both over a range of temperatures (10–40 °C) at constant shear rate (1 Hz) and at constant temperature (27 °C) over a range of shear rates (0.1–100 Hz) (Fig. 3b,c). Rheological analysis confirmed the stability of UDO₃-I as a liquid over all the explored range of temperatures, with viscosities ranging from over 100 Pa s at 10 °C to around 2 Pa s at 40 °C. At room temperature, UDO₃-I displayed a viscosity of 10 Pa s which was observed to be not dependent on the shear rate, suggesting an ideal Newtonian behavior characteristic of small molecular liquids. Unlike previously reported methacrylated diurethanediols and the herein presented UDO₂-I, the liquid form of UDO₃-I makes

Fig. 3 Spectroscopic and rheological characterization of UDO$_3$-I. **a** ATR–FTIR spectrum with the assignment of the most characteristic absorption bands; **b** viscosity as a function of temperature at constant shear rate (1 Hz); **c** viscosity as a function of shear rate at constant temperature (27 °C)
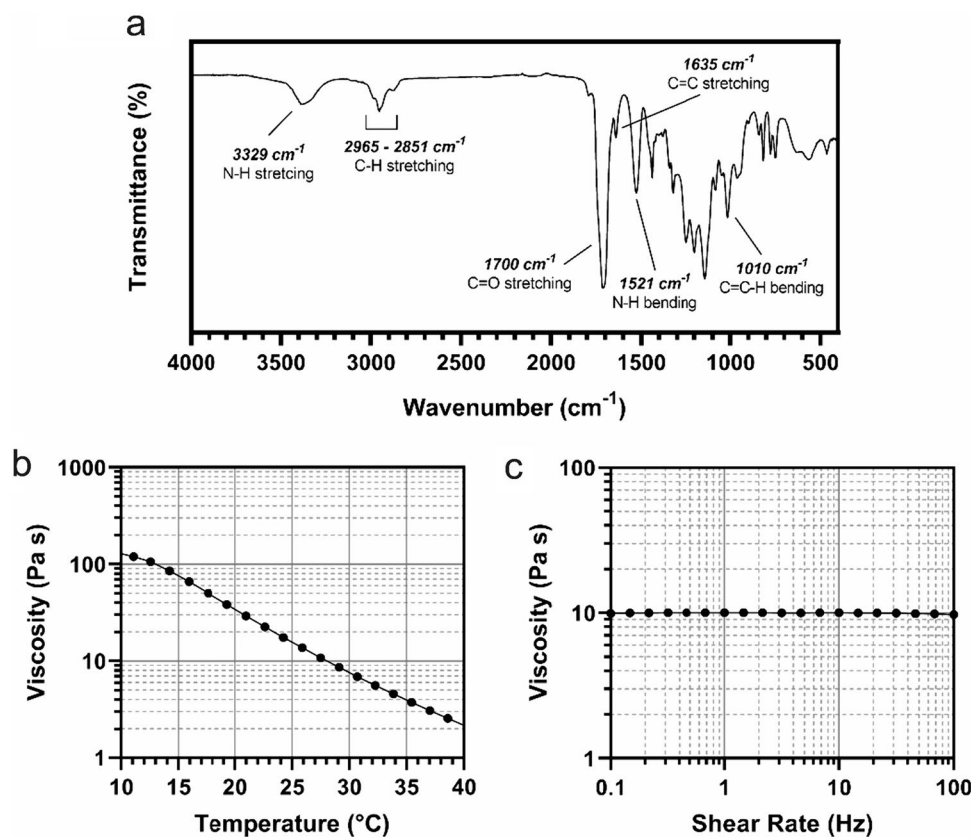
it possible for its formulation in photocurable resins with virtually no limit related to its solubility with the other monomeric components, and therefore expanding its applicability for such purposes. In fact, the high polarity and strong H-bonding capabilities of the carbamate group strongly limit its solubility in organic mixture such as those composed of photopolymerizable monomers. While this is not the first ever reported example of liquid bifunctional photocurable diurethane, it has to be underlined that such examples are always produced using isocyanates and are characterized by very low biobased content and sustainability. Therefore, the presented UDO$_3$-I represent the first biobased liquid bifunctional photocurable diurethane ever reported, so far. To support the claimed advantages of liquid diurethanes compared to their solid counterparts, the prepared UDO$_2$-I and UDO$_3$-I were then formulated with photocurable monomers for the preparation of resins for VP. However, it was immediately clear that UDO$_2$-I displayed very little solubility in the selected monomer mixtures, while UDO$_3$-I could be mixed virtually in all proportions (Table 1). In fact, no more than 5 wt.% of UDO$_2$-I could be efficiently dissolved into the resins; since the increase in biobased content of photocurable mixtures would not be significantly altered by such a small amount of added UDO$_2$-I, its applicability as VP monomer was not explored any further.

A first set of resin was prepared by mixing UDO$_3$-I with a 1:1 mixture of glycerol dimethacrylate (GDMA, mixture of isomers) and glycerol propoxylate triacrylate (GPT, average $M_n = 428$), to evaluate its effect on the mechanical properties of fossil-based (meth)acrylate formulations while increasing their biobased contents (resins A0–A3). Then, resins with higher biobased contents were prepared by employing the bifunctional itaconic acid-based reactive diluent 1,4-butanediol bis(methyl itaconate) (named I$_2$B$_1$) as a partial replacement of the mixture of glycerol-based photocurable monomers (resins B0 and C0). Finally, UDO$_3$-I was introduced at 50 wt.% on such formulations, to evaluate once again its effect on their mechanical properties (resins B1 and C1). This is the highest attempted loading of non-isocyanate urethane-based photocurable components for VP, and it has been possible thanks to the liquid state of UDO$_3$-I at room temperature. In addition to the photopolymerizable component, all formulations contained a photoinitiator (ethyl phenyl (2,4,6-trimethylbenzoyl) phosphinate Et-APO, 2 wt.%), a radical inhibitor (2,6-diterbutyl-4-methylphenol, BHT, 0.5 wt.%), and a photosensitizer (2-isopropyl thioxanthone, ITX, 0.3 wt.%). Moreover, a biobased plasticizer (Grinsted Soft-N-Safe, SNS, 7.2 wt.%) was added to each mixture. The biobased content of the prepared formulations was evaluated by calculating for each component of the resin the percentage of their molecular weight that is

composed of building block of renewable derivation. In particular, itaconic acid-based monomers and the plasticizer SNS were characterized by 100% biobased derivation, while the photoinitiating system was considered fully non-renewable. For the glycerol-based monomeric components GDMA and GPT, their biobased contents were calculated to be equal to 32.4% and 17.3%, respectively, considering as fully biobased their glycerol core. This approach has allowed to calculate the biobased contents for each formulation (Table 1). All resins were efficiently printed into 3D shapes with high spatial accuracy and resolution, also supporting the addition of small amounts of a natural dye (purpurin, 0.005 wt.%) to print colored 3D objects (Fig. 4). Furthermore, with each formulation, tensile and flexural test specimens were printed and tested according to the specifications for ISO 37 Type 2 and ISO 178, respectively. Due to the well-known lower reactivity of itaconic acid residues when compared to acrylates and methacrylates with respect to radical polymerization, the replacement of commercially available non-biobased urethane methacrylates with UDO3-I, and other itaconic acid-based reactive diluents require a re-optimization of instrumental printing parameters. In our case, the employed LCD 3D printing technology limited

the explorable parameters to the exposure time per layer, which was increased to up to 2 min every 0.1 mm of object height (Table 2). However, more advanced implementations allow for the optimization of additional parameters such as light power, with the aim of reducing the lengthening of the 3D printing process caused by the presence of biobased components.

From the tensile and flexural stress–strain curves (Figure S8-S9), the main mechanical properties of the 3D printed materials were extracted, collected in Table 2, and summarized in Fig. 5. By taking into consideration the first group of 3D printed materials (resins A0–A3) composed of increasing amounts of UDO_3-I in a 1:1 mixture of GPT and GDMA, its effect is immediately evident. The gradual replacement of the glycerol (meth)acrylate mixture with UDO_3-I lead to a continuous decrease in the elastic modulus, with subsequent increase of the elongation at break and an overall improvement of the mechanical properties represented by the increasing tensile strength, up to a UDO_3-I loading of 30 wt.% (corresponding to resin A2). However, when the loading was increased to 50 wt.% (resin A3), a drop in elongation at break and tensile strength was recorded, revealing a limit

Fig. 4 Digital camera picture of high-resolution 3D printed objects. **a** Tensile test specimens obtained by printing resins A3, B2 and C2 (from left to right). **b**, **c** Small lizard ($60 \times 35 \times 25$ mm³), watch strap and a stag, printed with resin C2. Details of the stag's antlers are smaller than 1 mm and clockface dimensions are $40.5 \times 35.8 \times 8.95$ mm, to serve as a reference
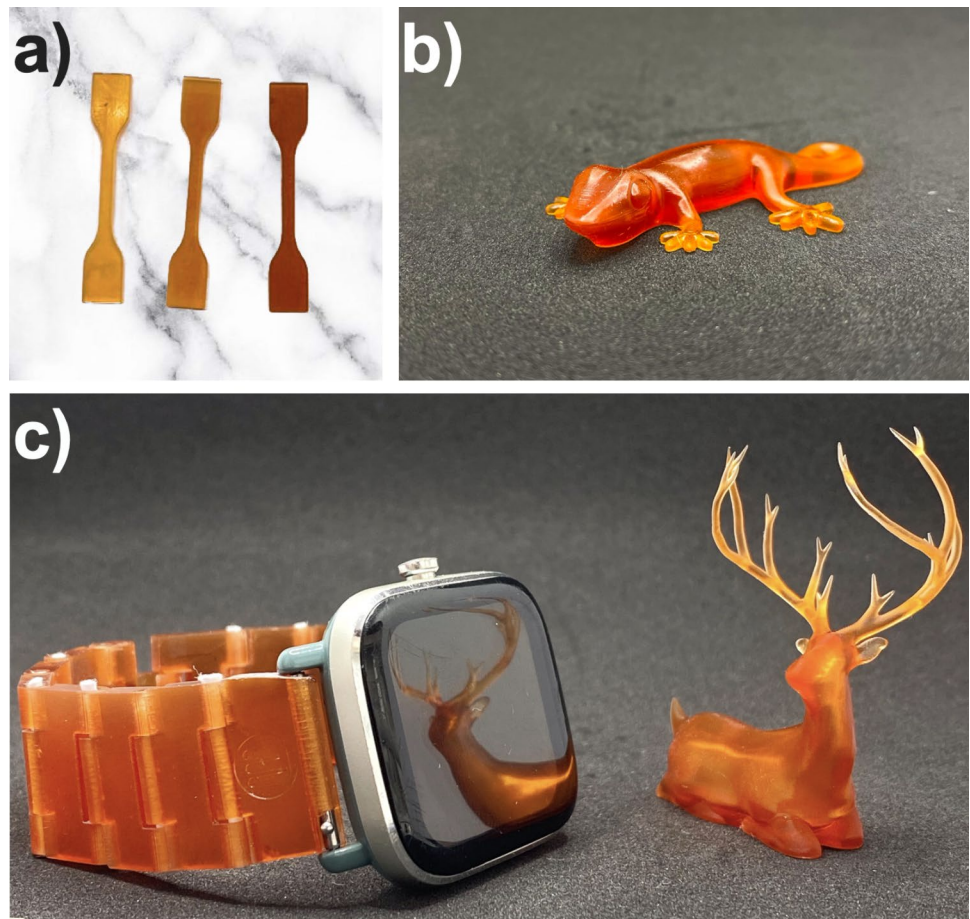
Table 2 Tensile, flexural, and hardness properties of 3D printed materials and the comparison for some reported data on commercially available resins. Data are expressed as mean ± SD obtained on four replicate measurements

Resin	Elastic modulus (GPa)	Elongation at break (%)	Tensile strength (MPa)	Flexural modulus (GPa)	Deformation at break (%)	Flexural strength (MPa)	Hardness (shore D)	Irradiation time (s/ layer)
A0	1.25 ± 0.26	1.8 ± 0.8	22.6 ± 9.7	2.54 ± 0.17	3.2 ± 0.4	76.5 ± 6.4	89 ± 1	120
A1	1.20 ± 0.07	3.6 ± 0.8	31.4 ± 3.7	2.60 ± 0.09	2.7 ± 0.3	63.3 ± 7.4	88 ± 1	80
A2	0.904 ± 0.115	3.7 ± 0.5	31.3 ± 3.9	2.42 ± 0.15	3.3 ± 0.4	67.3 ± 5.5	87 ± 1	80
A3	0.685 ± 0.044	1.60 ± 0.3	10.6 ± 1.9	1.01 ± 0.14	3.5 ± 0.3	30.2 ± 2.7	80 ± 1	110
B0	1.19 ± 0.08	1.9 ± 0.4	19.3 ± 2.5	2.49 ± 0.13	3.1 ± 0.5	66.7 ± 6.7	88 ± 1	80
B1	1.01 ± 0.11	6.2 ± 1.2	44.2 ± 2.7	2.24 ± 0.07	3.4 ± 0.1	67.5 ± 1.9	87 ± 1	110
C0	1.02 ± 0.08	0.80 ± 0.1	8.5 ± 1.2	2.57 ± 0.13	2.9 ± 0.3	72.0 ± 7.1	88 ± 1	80
C1	0.910 ± 0.025	4.0 ± 0.4	30.9 ± 2.7	2.15 ± 0.13	1.8 ± 0.3	39.9 ± 6.7	83 ± 1	120
Phrozen-speed	0.9	20	25	–	–	–	79	–
SUNLU 3000G	0.65	5	20	–	–	–	80	–

Fig. 5 Tensile and flexural properties of 3D printed materials. Plotted data are reported in Table 2
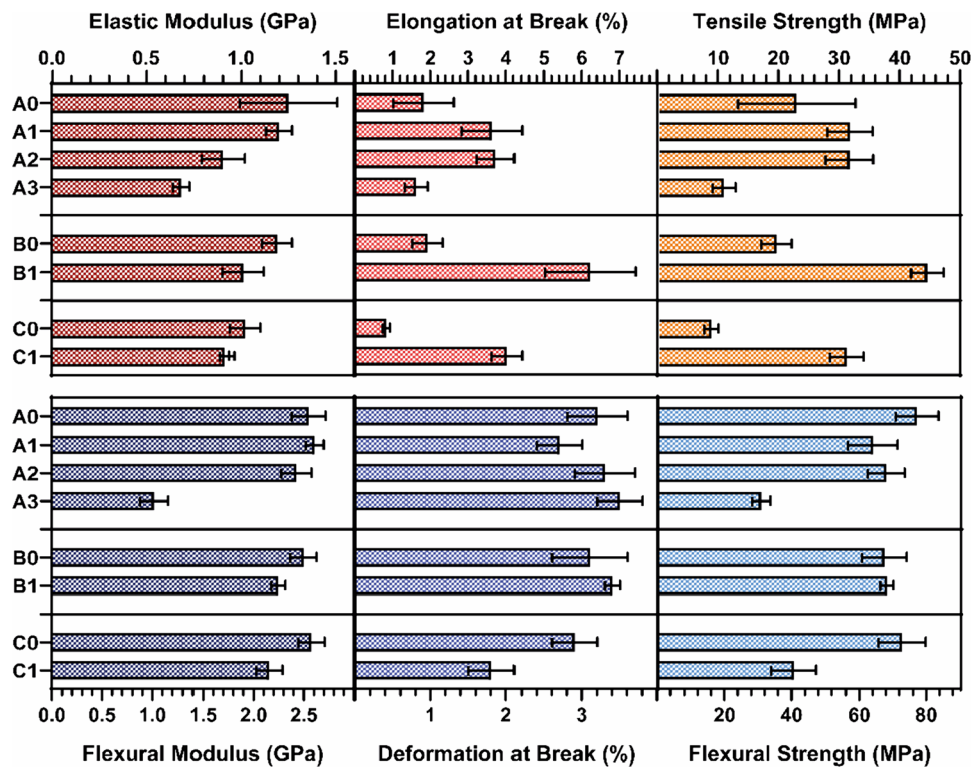
in the performances of UDO_3-I as a monomer, when formulated with GPT and GDMA. To verify this assumption, GPT and GDMA were partially and almost completely replaced with the biobased cross-linker I_2B_1 and printed with and without the presence of 50 wt.% UDO_3-I (resins B0–C1). The tensile testing of such materials revealed that the addition of the butanediol-based reactive diluents was able to amplify the effect of UDO_3-I on the mechanical properties; in fact, the addition of 50 wt.% UDO_3-I to a resin composed of GPT, GDMA, and I_2B_1 in 3:3:2 proportion (resin B1 vs B0) caused a limited decrease in the

elastic modulus (− 15%) and a significant increase in elongation at break (+ 226%) and tensile strength (+ 129%). This effect is even more evident when the resin composition is changed to higher I_2B_1 contents (resin C1 vs C0), where the GPT, GDMA, and I_2B_1 are changed to 1:1:6. In this case, the addition of UDO_3-I caused a less notable decrease in the elastic modulus (− 11%) accompanied by a remarkable increase in elongation at break (+ 400%) and tensile strength (+ 264%). It is worth underlining that resin C1 is the first ever reported resin with a biobased content as high as 89.7 wt.% displaying tensile modulus

almost reaching 1 GPa and tensile strength above 30 MPa, being therefore able to serve as a promising candidate for the formulation and the production of biobased resins for VP able to display improved properties compared to many fossil-based counterparts. The flexural properties, on the other hand, do not seem to depend strongly on the resin's composition, except for two isolated cases. Resin A3 displayed a strong reduction in flexural strength related to a significant decrease in its flexural modulus, while resin C1 still showed reduced flexural strength but, this time, related to a reduction in the deformation at break, with a slight observed increment in the flexural modulus. It is crucial, however, to keep in mind the intrinsic anisotropy of 3D printed materials, especially when evaluating their mechanical properties. In fact, during tensile testing the mechanical stress is applied along the photocured layers, with virtually no component laying perpendicular to it, and therefore the interlayer adhesion gives little to no contribution to the tensile properties. On the other hand, in this configuration, three-point flexural testing generates compressive and tensile stresses perpendicular to the layer planes and consequently the flexural properties are more related to interlayer adhesion. Therefore, the comparison between tensile and flexural properties is not trivial, as they describe different aspects of the materials' mechanical behavior. While UDO_3-I demonstrated to act as a softening agent that reduces rigidity and increases deformability under tensile stress with an overall improvement of the materials' strength in all tested formulations except A3, its effectiveness on the flexural properties is limited. Furthermore, the formulation in which UDO_3-I showed the most relevant improvement in tensile properties (resin C1) is also the one that suffered most significantly from the flexural point of view. Finally, with respect to hardness, all materials displayed hardness in the 80–90 Shore D range, following the trend observed for the elastic modulus, as can be expected from photocured thermosets. Finally, when compared to commercially available resins based on urethane diacrylates, the proposed biobased resins display comparable elastic modulus, generally lower elongation at break and often higher tensile strength, therefore underlining the potential of UDO_3-I as a viable replacement for isocyanate-based urethane photocurable monomer for high-performance additive manufacturing. Because of their similarity with commercially available alternatives, their typical applications are those associated with this class of materials, ranging from general merchandise to high-value products such as jewelry and textiles, but representing a significant step toward the improvement of sustainability in the 3D printing industry.

4 Conclusions

In conclusion, the presented approach described the preparation of biobased and photocurable diurethanediols bis(methylitaconate) named UDOs-I by aminolysis of cyclic carbonates and further functionalization with itaconic acid monomethyl ester, to be employed as monomers for the formulation of biobased resins for VP. While the use of symmetric ethylene carbonate led to a solid compound (UDO_2-I) that could not be efficiently formulated into photocurable mixtures, our objective was the introduction of asymmetry using propylene carbonate that hindered the solidification of the mixture, allowing for the obtainment of a liquid monomer (UDO_3-I) that could be easily formulated for the first time with (meth)acrylic and itaconic acid-based co-monomers in all proportions. By analyzing the materials in terms of their tensile and flexural properties, it was possible to conclude that resins formulated with up to 50 wt.% UDO_3-I and I_2B_1 displayed mechanical properties that are better or equal to the ones of the (meth)acrylate-based formulations, this suggests the remarkable potential of this kind of biobased photocurable monomers for increasing the sustainability of the VP manufacturing process. Finally, resins B1 and C1 are the first ever reported example of a resin for VP associated with a biobased content as high as 75 wt.% and 90 wt.% that are able to be photocured into solid materials showing tensile strength around 1 GPa. At present, there are no biobased resins that can entirely supplant acrylate- and methacrylate-based formulations in terms of both printability and mechanical properties. Nonetheless, researchers are making headway in this domain by creating fresh monomers, for instance, UDO_3-I, which can enable the formulation to have a higher biobased content while maintaining its performance. This advancement presents a viable avenue for industrial producers to enhance their sustainability practices.

Declarations

Conflict of interest On behalf of all authors, the corresponding author states that there is no conflict of interest.

References

1. Gibson I, Rosen D, Stucker B (2015) Additive Manufacturing Technologies, 2nd. Springer, New York
2. Chua CK, Leong KF, Lim CS (2003) Rapid Prototyping. World Scientific, Singapore
3. Shahrubudin N, Lee TC, Ramlan R (2019) An overview on 3D printing technology: technological, materials, and applications. Procedia Manuf 35:1286–1296. https://doi.org/10.1016/j.promfg.2019.06.089
4. Attaran M (2017) The rise of 3-D printing: The advantages of additive manufacturing over traditional manufacturing. Bus Horiz 60:677–688. https://doi.org/10.1016/j.bushor.2017.05.011
5. Schmidleithner C, Kalaskar DM, Schmidleithner C, Kalaskar DM (2018) Stereolithography. 3D Print. https://doi.org/10.5772/INTECHOPEN.78147
6. Bártolo PJ (2011) Stereolithographic processes. In: Bártolo PJ (ed) Stereolithography. Springer, US, Boston
7. Berglund G, Tkaczyk T (2021) Entirely 3D printed spectrometer: application of consumer-grade printing technologies for fabrication of optical and opto-mechanical components. In: Frontiers in optics + laser science 2021. Optica Publishing Group, Washington, D.C., p FM3C.6
8. Wegmüller L, Halbeisen F, Sharma N et al (2021) Consumer vs. high-end 3D printers for guided implant surgery—an in vitro accuracy assessment study of different 3D printing technologies. J Clin Med 10:4894. https://doi.org/10.3390/jcm10214894
9. Kaza A, Rembalsky J, Roma N et al (2018) Medical applications of stereolithography: an overview. Int J Acad Med 4:252. https://doi.org/10.4103/IJAM.IJAM_54_18
10. Liu B, Gong X, Chappell WJ (2004) Applications of layer-by-layer polymer stereolithography for three-dimensional high-frequency components. IEEE Trans Microw Theory Tech 52:2567–2575. https://doi.org/10.1109/TMTT.2004.837165
11. Mukhtarkhanov M, Perveen A, Talamona D (2020) Application of stereolithography based 3D printing technology in investment casting. Micromachines 11:946. https://doi.org/10.3390/mi11100946
12. Arif ZU, Khalid MY, Noroozi R et al (2022) Recent advances in 3D-printed polylactide and polycaprolactone-based biomaterials for tissue engineering applications. Int J Biol Macromol 218:930–968. https://doi.org/10.1016/j.ijbiomac.2022.07.140
13. Tariq A, Arif ZU, Khalid MY et al (2023) Recent advances in the additive manufacturing of stimuli-responsive soft polymers. Adv Eng Mater. https://doi.org/10.1002/adem.202301074
14. Deng Y, Li J, He Z et al (2020) Urethane acrylate-based photosensitive resin for three-dimensional printing of stereolithographic elastomer. J Appl Polym Sci 137:49294. https://doi.org/10.1002/app.49294
15. Pitzanti G, Mohylyuk V, Corduas F et al (2023) Urethane dimethacrylate-based photopolymerizable resins for stereolithography 3D printing: a physicochemical characterisation and biocompatibility evaluation. Drug Deliv Transl Res. https://doi.org/10.1007/s13346-023-01391-y
16. Sinh LH, Harri K, Marjo L et al (2016) Novel photo-curable polyurethane resin for stereolithography. RSC Adv 6:50706–50709. https://doi.org/10.1039/C6RA05045J
17. Stachak P, Łukaszewska I, Hebda E, Pielichowski K (2021) Recent advances in fabrication of non-isocyanate polyurethane-based composite materials. Materials (Basel) 14:3497. https://doi.org/10.3390/ma14133497
18. Ghasemlou M, Daver F, Ivanova EP, Adhikari B (2019) Bio-based routes to synthesize cyclic carbonates and polyamines precursors of non-isocyanate polyurethanes: a review. Eur Polym J 118:668–684. https://doi.org/10.1016/j.eurpolymj.2019.06.032
19. Błażek K, Beneš H, Walterová Z et al (2021) Synthesis and structural characterization of bio-based bis(cyclic carbonate)s for the preparation of non-isocyanate polyurethanes. Polym Chem 12:1643–1652. https://doi.org/10.1039/D0PY01576H
20. Liu Q, Wu L, Jackstell R, Beller M (2015) Using carbon dioxide as a building block in organic synthesis. Nat Commun 6:5933. https://doi.org/10.1038/ncomms6933
21. Wai PT, Jiang P, Shen Y et al (2019) Catalytic developments in the epoxidation of vegetable oils and the analysis methods of epoxidized products. RSC Adv 9:38119–38136. https://doi.org/10.1039/C9RA05943A
22. Huang K, Ling Z, Zhou Q (2021) Urethane diols through non-isocyanate approach and their application in MF coating. J Compos Sci 5:194. https://doi.org/10.3390/jcs5070194
23. Báez JE, Ramírez D, Valentín JL, Marcos-Fernández Á (2012) Biodegradable poly(ester–urethane–amide)s based on poly(ε-caprolactone) and diamide-diol chain extenders with crystalline hard segments. Synth Charact Macromol 45:6966–6980. https://doi.org/10.1021/ma300990s
24. Wang X, Gao S, Wang J et al (2021) The production of biobased diamines from renewable carbon sources: current advances and perspectives. Chin J Chem Eng 30:4–13. https://doi.org/10.1016/j.cjche.2020.12.009
25. Singh N, Bakhshi H, Meyer W (2020) Developing non-isocyanate urethane-methacrylate photo-monomers for 3D printing application. RSC Adv 10:44103–44110. https://doi.org/10.1039/D0RA06388F
26. Willke T, Vorlop K-D (2001) Biotechnological production of itaconic acid. Appl Microbiol Biotechnol 56:289–295. https://doi.org/10.1007/s002530100685
27. Pérocheau Arnaud S, Malitowski NM, Meza Casamayor K, Robert T (2021) Itaconic acid-based reactive diluents for renewable and acrylate-free UV-curing additive manufacturing materials. ACS Sustain Chem Eng 9:17142–17151. https://doi.org/10.1021/acssuschemeng.1c06713
28. Maturi M, Pulignani C, Locatelli E et al (2020) Phosphorescent bio-based resin for digital light processing (DLP) 3D-printing. Green Chem 22:6212–6224. https://doi.org/10.1039/D0GC01983F
29. Vetri Buratti V, Sanz de Leon A, Maturi M et al (2022) Itaconic-acid-based sustainable poly(ester amide) resin for stereolithography. Macromolecules 55:3087–3095. https://doi.org/10.1021/acs.macromol.1c02525
30. Maturi M, Spanu C, Maccaferri E et al (2023) (Meth)acrylate-free three-dimensional printing of bio-derived photocurable resins with terpene- and itaconic acid-derived poly(ester-thioether)

s. ACS Sustain Chem Eng 11:17285–17298. https://doi.org/10.1021/acssuschemeng.3c04576

31. Han L, Dai J, Zhang L et al (2014) Diisocyanate free and melt polycondensation preparation of bio-based unsaturated poly(ester-urethane)s and their properties as UV curable coating materials. RSC Adv 4:49471–49477. https://doi.org/10.1039/C4RA08665A

32. Froidevaux V, Negrell C, Caillol S et al (2016) Biobased amines: from synthesis to polymers; present and future. Chem Rev 116:14181–14224. https://doi.org/10.1021/acs.chemrev.6b00486

33. Nohra B, Candy L, Blanco J-F et al (2012) Aminolysis reaction of glycerol carbonate in organic and hydroorganic medium. J Am Oil Chem Soc 89:1125–1133. https://doi.org/10.1007/s11746-011-1995-5

34. Olsén P, Oschmann M, Johnston EV, Åkermark B (2018) Synthesis of highly functional carbamates through ring-opening of cyclic carbonates with unprotected α-amino acids in water. Green Chem 20:469–475. https://doi.org/10.1039/C7GC02862H

35. Spanu C, Locatelli E, Sambri L et al (2024) Photocurable itaconic acid-functionalized star polycaprolactone in biobased formulations for vat photopolymerization. ACS Appl Polym Mater. https://doi.org/10.1021/acsapm.3c03159